Porous composite biomaterials based on silicon nitride and bioglass

Františka Frajkorová[1,a*], KatarínaBodišová[2,b], Martin Boháč[1,c],
EvaBartoníčková[1,d], Jaroslav Sedláček[3,e]

[1] Faculty of Chemistry, Brno University of Technology, Purkyňova 464/118, 612 00 Brno, CzechRepublic
[2] Department of Ceramics, Glass and Cements, Faculty of Chemical and Food Technology, Slovak University of Technology in Bratislava, Radlinského 9, 812 37 Bratislava, Slovak Republic
[3] Institute of Inorganic Chemistry, Slovak Academy of Sciences, 84536 Bratislava, Slovak Republic
[a]frajkorova@fch.vutbr.cz, [b] qghillanyova@stuba.sk, [c]bohac@fch.vutbr.cz, [d] bartonickova@fch.vutbr.cz,[e] jaroslav.sedlacek@savba.sk

Keywords: Sintering, Composites, Glass, Nitrides, Biomedicalapplications

Abstract

The combination of bioinert and bioactive material offers new potentialities in bone tissue engineering. The present paper deals with preparation of novel biomaterial composite based on silicon nitride (Si_3N_4) and bioglass (in amount of 10 and 30 wt%) by free sintering at 980 °C for 1h in nitrogen atmosphere. The obtained material was characterized by differential thermal analysis (DTA) and X-ray powder diffraction (XRD). The bioactivity was examined *in vitro* with respect to the ability of hydroxyapatite layer formation on the surface of materials as a result of contact with simulated body fluid (SBF). All composites were studied by Fourier transform infrared spectroscopy (FTIR) and scanning electron microscopy (SEM) before and after immersion in SBF. Thebioglass-free sample was prepared as a reference material to compare the microstructure and bioactivity to the composites.

1. Introduction

Silicon nitride (Si_3N_4) based ceramics represent a combination of mechanical, tribological, thermal and chemical properties that makes them suitable for high performance components in severe environments in several industrial applications. These properties, namely hardness, fracture toughness, friction and wear coefficient, are also very important for many high-load medical application of bioceramics in the human body. Another desirable property of ceramic-based implants is bioactivity.

On the basis of potentialities, silicon nitride attracts interest for orthopedic and dental applications [1-7] in the human body, but is not yet established as a biomaterial in medicine. This is related to some controversy in the literature about the biocompatibility [1,4-6]. Several works on biocompatibility and bioactivity of silicon nitride outline that silicon nitride based ceramics can be used as materials for clinical applications in the field of hard tissue surgery. The absence of toxic behaviour was ascertained during toxicity tests [8].

In the application of silicon nitride as a biomaterial a key aspect is the presence of grain boundary phases deriving from the necessary use of sintering aids. The grain boundary phasecomposition and amount depend on the selected additives which, during sintering, react with the silica presents on

the silicon nitride particles and other impurities, leading to the formation of a liquid phase. This allows the sintering of silicon nitride, but the final dense ceramics contains amorphous or partially crystalline grain boundary phases. It has to be taken into account that the glassy phases may exhibit bioactivity different from silicon nitride crystalline phases. Generally used additives for sintering of silicon nitride there are Mg, Al, rare earthand bioactive glass as novel sintering aid [9].

The first bioactive material reported was a four component glass composed of SiO_2, CaO, Na_2O, and P_2O_5 by Hench et al in 1971 [10]. Bioglass[®]45S5 has the following chemical composition: 45.0 SiO_2–24.5 Na_2O –24.5 CaO–6.0 P_2O_5 in wt%. It is a silicate glass based on the 3-D glass forming SiO_2 network in which Si is fourfold coordinated to O. The key compositional features that are responsible for bioactivity of 45S5 glass are its low SiO_2 content (compared to more chemically durable silicate glasses), high Na_2O and CaO (glass network modifiers) content and high CaO/ P_2O_5 ratio [11]. When implanted, the low silica content and the presence of sodium ions in the glass results in very rapid ion exchange with the protons and hydronium ions of physiological solutions [12]. The ion exchange creates an alkali pH at the implant interface with the body fluids, leading to nucleation and crystallisation of hydroxyl carbonate apatite (HCA) bone mineral at the surface of the glass. The growing bone mineral layer bonds to collagen, produced by the bone cells, and forms a strong interfacial bond between the implant and the living tissue [13,14].

However, medical applications of bioglass have been centred on low stress fields, mainly due to its non-adequate fracture toughness compared to that of cortical bone. This limitation is unfortunately a common characteristic of glasses, ceramics and glass ceramics used in medical applications. Theoretically, Si_3N_4-bioglass composites would lead to medical implants that combine the advantageous properties of each material individually. Amaral, Santos et al. [3,15] have prepared almost fully dense Si_3N_4-bioglass composite by hot pressing technique with exceptional mechanical properties that make it suitable for high-load application.

The present work describes the preparation of porous bioactive composite, based on silicon nitride and 45S5 Bioglass[®],using free sintering. The pressureless sintering allows preparation of porous material by economic and simple way. A complete description of preparation, sinteringand microstructural characterization and also bioactivity is reported.

2. Experimental Procedure

Si_3N_4 –bioglass composites were prepared from a mixture of a Si_3N_4 commercial powder (Yantai, Tomley Hi-Tech Ind. &Tra. Co., Ltd., D_{90}=1.0 μm, O < 1.4%) and a bioglass. The bioglass (with the similar composition to Bioglass[®] 45S5) was prepared by sol-gel method according to the procedure [16] and has the following chemical composition: 45.0 SiO_2–24.5 Na_2O –24.5 CaO–6.0 P_2O_5 in wt%. The bioglass powder was then mixed with Si_3N_4 powder in a 0-30 % weight proportion in isopropanol by planetary milling for 2 h in a silicon nitride jar using silicon nitride balls. The homogenised suspension was dried and subsequently screened through 71 μm sieve in order to avoid large hard agglomerates. The pellets were uniaxially pressed at 100 MPa. The samples were free sintered at 980°C for 1h in nitrogen atmosphere. After the dwell time the samples were taken out from the furnace to inhibit the crystallisation of the bioglassas, according to Clupper and Hench [17-20], the crystal phase $Na_2Ca_2Si_3O_9$ slightly decreased the formation kinetics of an apatite layer on the Bioglass[®] sample surface but it did not totally suppress the formation of such a layer [20]. The sintering temperature of the composites was chosen on the basis of results obtained from the differential thermal analysis (DTA). The analysis was performed on TA Instruments Q600 equipment using a heating rate of 10°C/min and Al_2O_3 as reference.

The bioglass-free sample (referred as Si$_3$N$_4$-0) was prepared as a reference material to compare the microstructure and bioactivity to the composites. The sample was sintered in air at 1150 °C for 1h. The composition of studied systems are listed in Table 1.

Table 1. Chemical composition of studied systems.

Sample	Composition [wt%]	
	Si$_3$N$_4$	45S5 Bioglass®
Si$_3$N$_4$-0	100	0
Si$_3$N$_4$-10	90	10
Si$_3$N$_4$-30	70	30

The densities of the samples were measured by Archimedes method in water. The theoretical densities were calculated according to the rule of mixtures. The microstructure was observed by scanning electron microscopy (Zeiss, EVO 40 HV,Germany). The crystalline phases present in the ground samples were identified using X-ray diffraction (XRD) (Bruker AXS D8 Discover X-ray diffractometer).

The assessment of *in vitro* bioactivity was carried out by soaking samples in simulated body fluid (SBF) maintained at 36.5°C in incubation apparatus (Binder BD 115) for 7 and 21 days under a static regime. The SBF solution was preparedaccording to the standard procedure described by Kokubo and Takadama [21].After the soaking, the sample surface was characterized with scanning electron microscopy (Zeiss, EVO 40 HV, Germany) and Fourier transform infrared spectroscopy. The FTIR spectra were obtained using a Nicolet 6700 FTIR spectrometer from Thermo Scientific.The solutions were analysed using inductively coupled plasma optical emission spectrometer (ICP-OES) spectroscopy (HORIBA JY Ultima2) to determine the elemental concentration of Ca^{2+}, P^{5+} and Si^{4+} as a function of immersion time.

3. Results and Discussion

3.1 Thermal property analysis and phase characterisation

Fig. 1 shows the DTA curve of the Bioglass® powder prepared by sol-gel method. DTA curve presents two exothermic peaks, the first one at 305°C, the second one at 698°C and one endothermic effect in the region of 980-1030°C. Smaller exothermic peak at 305°C is probably a result of loss of residual organics from sol-gel process while large exothermic peak at 698°C corresponds to Bioglass® crystallisation. During the crystallisation process the development of new crystalline phase is detected. Theseresults are in agreement with those presented by Clupper and Hench [22]. Endothermic effect between 980 and 1030°C is attributed to glass transition region of bioglass, therefore the temperature of 980°C has been chosen as the sintering temperature. Bioglass at such a temperature acts as a sintering additive due to the transition of solid state to soften viscous liquid.
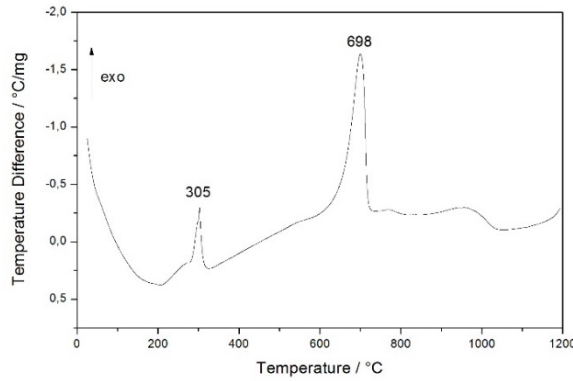
Fig. 1. DTA analysis of bioglass using a heating rate of 10°C/min.

The crystalline phase mentioned above is a sodium calcium silicate $Na_2Ca_2Si_3O_9$.X-ray powder patterns of Si_3N_4-composites are presented in Fig. 2. XRD phase analysis of the composite contains 30% of bioglass (Si_3N_4-30) confirmed the presence of $Na_2Ca_2Si_3O_9$ together with β- Si_3N_4 and SiO_2 (tridymit) as minority phases and α-Si_3N_4 as a majority phase.The XRD analysis of the composite contains 10% of bioglass (Si_3N_4-10)showed the presence of α-Si_3N_4 as a majority phase and β-Si_3N_4 and SiO_2 (cristobalite) as minority phases. The fact, that no further crystalline phases were not detected could indicate that no significant reactions occurred between silicon nitride and bioglass. However, the EDX analysis of the composite Si_3N_4-10 showed the presence of $Na_2Ca_2Si_3O_9$. It means that 45S5 bioglasshascrystallised to $Na_2Ca_2Si_3O_9$ but its concentration may be below the detection limit of XRD analysis.The XRD pattern of bioglass-free sample, Si_3N_4-0, sintered at 1150°C in air, is presented in Fig. 3. The results of phase analysis have revealed that α→β-Si_3N_4 phase transformation has occurred at sintering temperature, besides α-Si_3N_4 alsoβ- Si_3N_4, both hexagonal, was detected. The α→βphase transformation is proceeding through solution–diffusion–reprecipitation process [23].
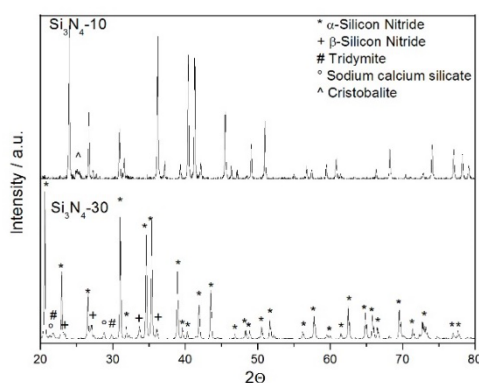

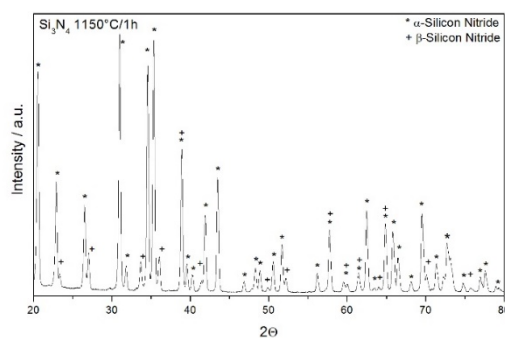Fig. 2. XRD pattern of the silicon nitride-bioglass composites, Si_3N_4-10 and Si_3N_4-30

Fig. 3. XRD pattern of the bioglass-free sample, Si_3N_4-0.

3.2 Microstructural characterisation

The values of densities, relative densities and porosity of the Si_3N_4-bioglass composites and bioglass-free sample are summarized in Table 2.

Table 2. Densities, relative densities and porosity of samples.

Sample	Density [g cm^{-3}]	Relative density [%]	Porosity [%]		
			Overall	Open	Close
Si$_3$N$_4$-0	1.7	52.5	47.5	40.1	7.4
Si$_3$N$_4$-10	1.9	60.3	39.7	33.9	5.9
Si$_3$N$_4$-30	2.0	65.7	34.3	24.0	10.3

From the results listed in the Table 2 is obvious that relative density of Si$_3$N$_4$-bioglass composites increases with the addition of bioglass. Relative densities of composites is higher in comparison with bioglass-free sample Si$_3$N$_4$-0 so it can be assumed that bioglass plays the role of sintering additive and promotes the sintering process of composites. However the changes in relative density as well as in porosity could have been more significantif the sintering temperature had been closer to the melting point of bioglass. Due to the lack of liquid phase which wets the solid grains of Si$_3$N$_4$ is not possible to speak about liquid phase sintering.

The microstructure of materials designed for bioapplications is of great importance.Overall porosity of the Si$_3$N$_4$-bioglass composites decrease with increased content of bioglass. This is in accordance with observed increasing density with the rising bioglass content. The porosity of the Si$_3$N$_4$-bioglass composites and bioglass-free sample was calculated using Archimedes method of weighing in water.

Complex microstructural characterisation offers SEM analysis. The micrographs of reference Si$_3$N$_4$-0 sample and as well as Si$_3$N$_4$-bioglass composites with 10 and 30% of bioglass are shown in Fig. 4. The final microstructures of Si$_3$N$_4$-bioglass composites shown in Fig. 4a), b) reveal irregularly distributed prolonged crystals of bioglass in α-Si$_3$N$_4$ matrix. With increasing content of bioglass in the composite also grows the amount of crystals with lath-like morphology overlapping the equiaxial α-Si$_3$N$_4$ grains. The microstructure of bioglass-free sample in Fig. 4c) shows a few elongated β- Si$_3$N$_4$ grains in matrix formed of equiaxial α-Si$_3$N$_4$ grains.
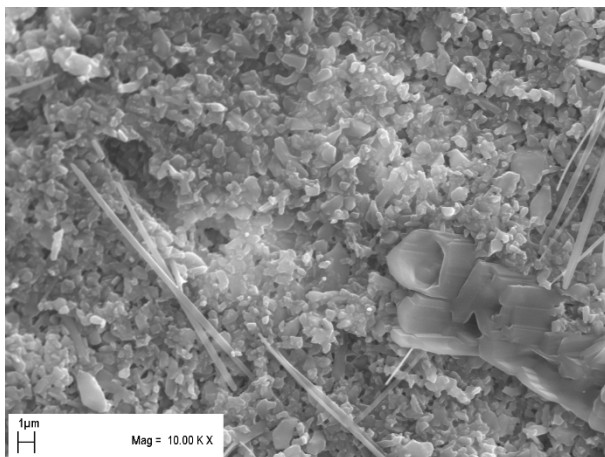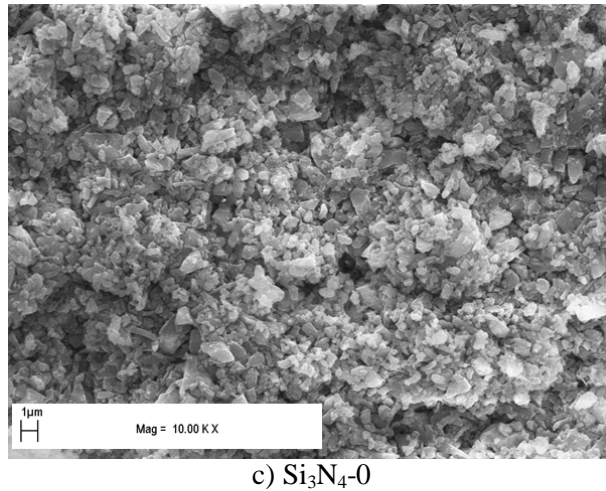

a) Si$_3$N$_4$-10
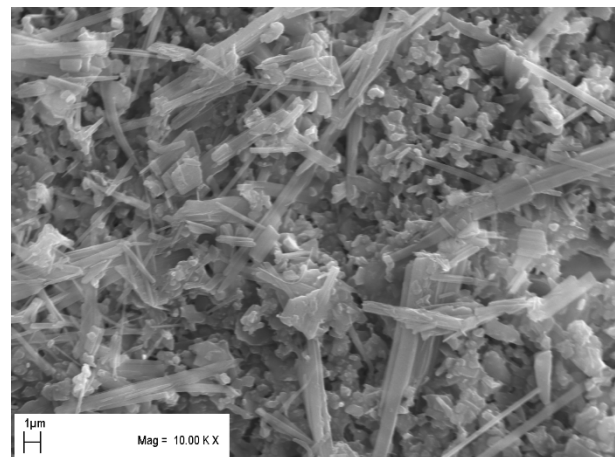
b) Si$_3$N$_4$-30

c) Si_3N_4-0

Fig. 4. The microstructures of Si_3N_4-bioglass composites with 10 a 30% of bioglass and reference bioglass-free sample (magnification x1000).

3.3 Bioactivity

In vivo bone bioactivity of a material can be predicted from the apatite formation on its surface in SBF. SEM micrographs of the surfaces of the Si_3N_4-bioglass composites after soaking in SBF for 7 (Fig. 5a), b))and 21 days (Fig. 6a), b)) show that the samples remained porous after a soaking period and the surface changes, typical for a bioactive material, can be observed. The morphological evolution in SBF follows a profile analogous to that reported for hydroxyapatite (HA) coatings [24]. After immersion for 7 day in SBF a newly formed hydroxyapatite plates of irregular shape are visible on the surface of sample Si_3N_4-10 (Fig. 5a)). As presented in Fig. 5b), after immersion for 7 days in SBF on the surface of sample Si_3N_4-30 locally grown small spherical hydroxyapatite granules. After soaking in SBF for 21 days, is the surface of sample Si_3N_4-10 almost totally covered with hydroxyapatite plates of irregular shape (Fig. 6a)), while the surface of sample Si_3N_4-30 is completely coated with HA film (Fig. 6b)) and the detailed picture revealed that the hydroxyapatite particles have spherical shape.

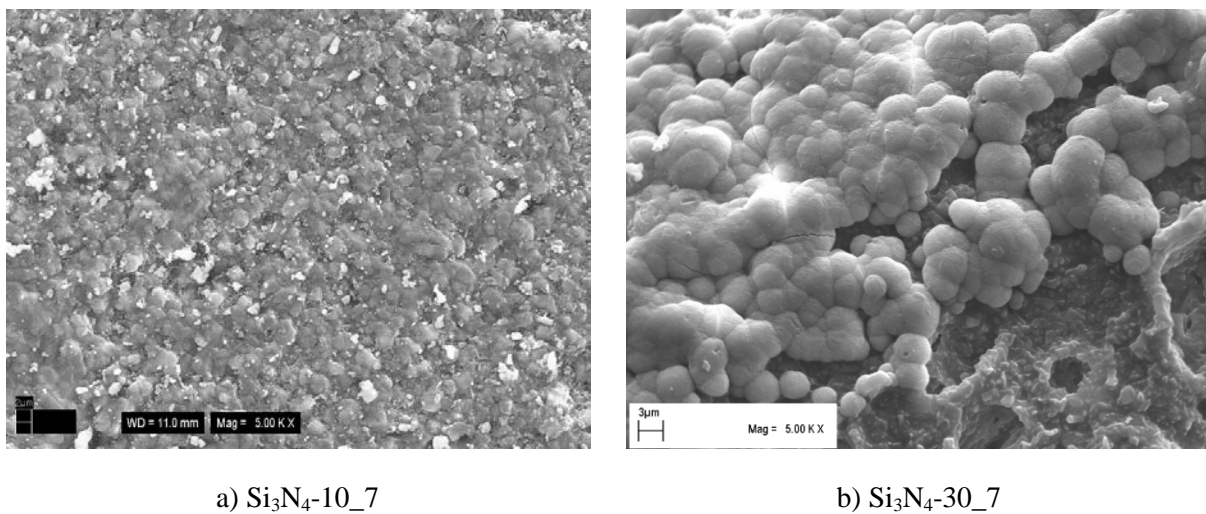a) Si_3N_4-10_7   b) Si_3N_4-30_7

Fig. 5. SEM micrographs showing the surface microstructure of the Si_3N_4-bioglass composites after soaking in SBF for 7 days (magnification 5000x):
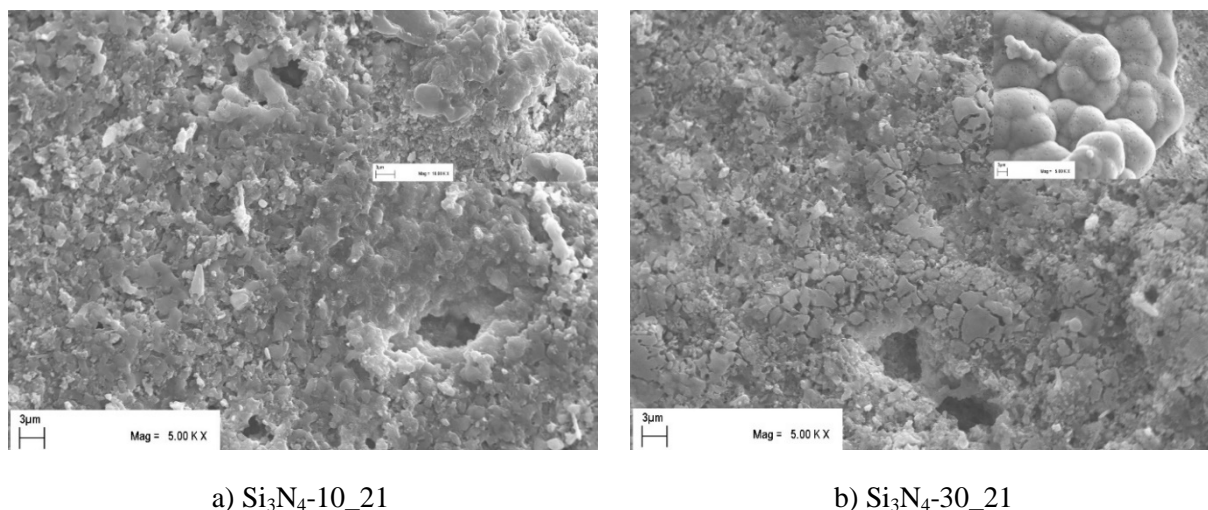
<div align="center">a) Si₃N₄-10_21   b) Si₃N₄-30_21</div>

a) Si_3N_4-10_21   b) Si_3N_4-30_21

Fig. 6. SEM micrographs showing the surface microstructure of the Si_3N_4-bioglass composites after soaking in SBF for 21 days (magnification 5000x). The surface details are shown in the pictures placed at the top-right corner of micrograph:

Control experiments in SBF were also performed with the bioglass-free sample Si_3N_4-0. In accordance with the expectations no surface changes, associated with the formation of hydroxyapatite, have occurred, as the silicon nitride is abioinert material.

3.4 Analysis of leachates

Examining the compositional change of SBF solution with time may provide insight into the mechanism of enhanced bioactivity of the Si_3N_4-bioglass composites. Fig. 7 - Fig. 9 show the changes in Ca^{2+}, P^{5+} and Si^{4+} concentration of the SBF as a function of soaking time, examined by ICP analysis. These results are very useful for understanding the phenomenon of ion transfer which takes place between the glass-ceramic surface and the synthetic physiological liquid. The variations of calcium concentration of the SBF after 7 and 21 days of immersion are shown in the Fig. 7. The marked release of Ca^{2+} ions into the SBF medium during 7 day test are due to partial dissolution of the surface. The concentration of Ca^{2+} ions increased from 2.5 mmol.dm^{-3} to 3.2 mmol.dm^{-3} in case of Si_3N_4-10 sample and from 2.5 mmol.dm^{-3} to 3.4 mmol.dm^{-3} for Si_3N_4-30 sample. After 21 days the concentration of Ca^{2+} decreased because SBF is already supersaturated with calcium ions regarding the HA formation. The decrease in the phosphorus concentrations, shown in Fig. 8, is likely due to the precipitation of the calcium phosphate layer, which consumes Ca^{2+} and P^{5+} ions from the SBF medium [25,26]. Changes in Ca^{2+} concentration correlated with changes in P^{5+} concentration and correspond to chemical composition of the composites. After 7 days test the concentration of P^{5+} fell from 1.0 mmol.dm^{-3} to 0.9 mmol.dm^{-3} for Si_3N_4-10 sample and from 1.0 mmol.dm^{-3} to0.8 mmol.dm^{-3} for Si_3N_4-30 sample. Regarding bioglass-free sample (Si_3N_4-0), the concentrations of Ca^{2+} and P^{5+} did not change, as silicon nitride is a bioinert material. As shown in Fig. 9, silicon concentration released into the SBF medium increases steadily with time of immersion in case of the composites and even in case of the bioglass-free Si_3N_4 sample, as silicon nitride grains are on their surface covered by a silica layer. The increase in Si^{4+} indicates the first stage of dissolution by the breaking of the outer silica layers of the network. The solid silica dissolves in the form of monosilicic acid $Si(OH)_4$ to the solution resulting from breaking of Si-O-Si

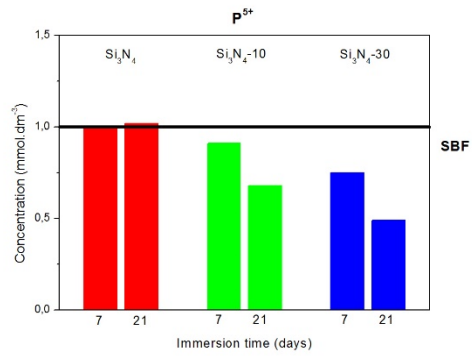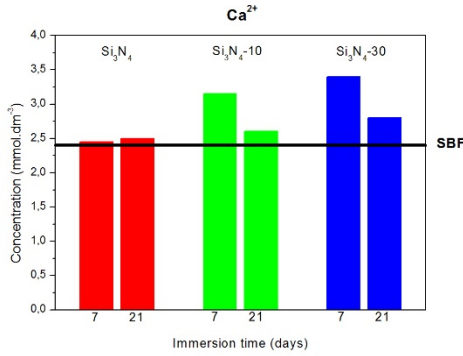bonds and formation of Si-OH (silanols) groups, which act as nucleation sites of the apatite layer [25].

Fig. 7. Variation of Ca^{2+} concentration in SBF after soaking the samples for 7 and 21 days.

Fig. 8. Variation of P^{5+} concentration in SBF after soaking the samples for 7 and 21 days.
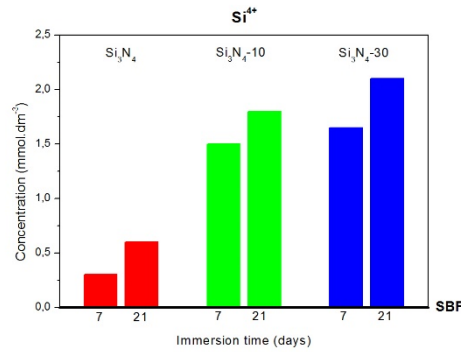

Fig. 9. Variation of Si^{4+} concentration in SBF after soaking the samples for 7 and 21 days

3.5 FTIR spectroscopy

In Fig. 10 and Fig. 11 can be seen FTIR spectra of composites with 10 and 30% of bioglass after 7 and 21 days of immersion in SBF. The presented spectra report the characteristic vibrations of silicon nitride, bioglass and newly formed hydroxyapatite. The most characteristic stretching vibration bands of silicon nitride were observed at 670 cm^{-1} (Si-N-Si) and at 880 cm^{-1} (Si-N). The group vibrations of Si-O-Si bending mode and Si-O stretching mode, in the regions of 550 cm^{-1} - 400 cm^{-1} and 1200 cm^{-1} - 850 cm^{-1} respectively are assigned to the nucleant agent, bioglass[27,28]. Bands at ~920 cm^{-1} and ~ 1030 cm^{-1} are attributed to P-O stretching vibration due to formation of hydroxyapatite (HA) layer on the surface of composites exposed to the SBF solution. Development of HA is also confirmed by the rise of peaks at ~560 cm^{-1} and ~ 590 cm^{-1} assigned to P-O bending vibration mode [29].

FTIR spectra of Si$_3$N$_4$-10 sample after 7 and 21 days of immersion in SBF, presented in Fig. 10 are almost identical while the spectra obtained from Si$_3$N$_4$-30 sample after 7 and 21 days in SBF (Fig 11) are slightly different. The characteristic peak of HA near 560 cm^{-1} belongs to the P-O bending vibration becomes stronger after 21 days test (solid curve) and is shifted to the characteristic peak position of pure HA (560 cm^{-1}).
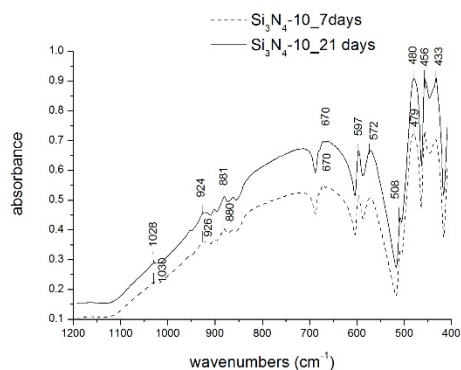
Fig. 10. FTIR spectra of Si₃N₄-10 sample after 7 (dashed curve) and 21 days (solid curve) of immersion in SBF.
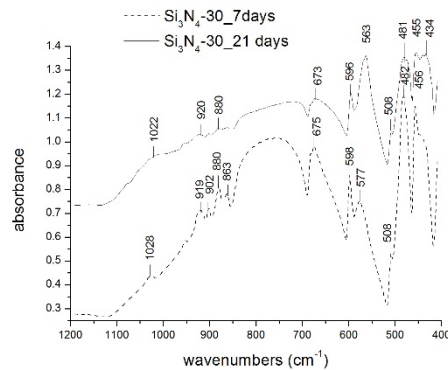
Fig. 11. FTIR spectra of Si₃N₄-30 sample after 7 (dashed curve) and 21 days (solid curve) of immersion in SBF.

4. Conclusion

Novel Si_3N_4 – bioglass composites (with 10 and 30 wt% of bioglass) were prepared using free sintering at 980 °C. Bioglass, with the similar composition to Bioglass® 45S5, was prepared using sol-gel method. Bioactive glass plays the role of sintering additive which partially supports the sintering of composite but mainly promotes the bioactivity of prepared materials. The bioactive behavior was confirmed by immersion of composites in simulated body fluid for different time period whereby the hydroxyapatite layer was developed on their surface. The presence of the hydroxyapatite was assessed by means of SEM and FTIR and also ICP analysis of the leachates shown the changes in Ca^{2+}, P^{5+} and Si^{4+} concentration of the SBF due to the hydroxyapatite formation. The bioglass-free sample prepared as a reference material exhibited no bioactivity which clearly confirmed the positive effect of bioglass addition.

References

[1]   C.C. Sorell, P.H. Hardcastle, R.K. Druitt, E.R. Mc Cartney, in: A. Ravaglioli, A. Krajewski (Eds.), Proceedings 5th Meeting and seminar on: Implants for spine, ceramics, cell and tissue annual conferences, ISTEC-CNR, Faenza, Italy, 1999, pp. 47.

[2]   Y.S. Zhou, K. Ikeuchi, M. Ohashi, Comparison of the friction properties of four ceramic materials for joint replacements, Wear 210 (1997) 171-177.

[3]   M. Amaral, M. A. Lopez, R.F. Silva, J.D Santos, Densification route and mechanical properties of Si₃N₄-bioglass biocomposites, Biomaterial 23 (2002) 857-862.

[4]   H.R Maier, C. Ragoss, M. Held, T. Reske, A. Neumann, K. Jahnke, Design and biocompatibility aspects of a minifixation system from Si₃N₄ for osteosynthesis, cfi/Ber. DKG81(2004) 33-38.

[5]   Y.S. Zhou, N. Tomita, K. Ikeuchi, M. Ohashi, K. Takashima, Study on the possibility of silicon nitride – silicon nitride as a material for hip prostheses, Mater. Sci. Eng.: C 5 (1977) 125-129.

[6]   A. Neumann, M. Kramps, C. Ragoss, H. R. Maier, K. Jahnke, Histological and microradiographic appearances of silicon nitride and aluminium oxide in a rabit femur implantation model, Materialwiss. Werkst. 35 (2004) 569-573.

[7]   K. Olsson, J. Li, L. Urban, EP Patent No. 1064238, 2003.

[8] C.C. Guedes e Silva, O.Z. Higa, J.C. Bressiani, Cytotoxic evaluation of silicon nitride based ceramics, Mater. Sci. Eng.: C 24 (2004) 643-646.

[9] M. Mazzochi, A. Bellosi, On the possibility of silicon nitride as a ceramic for structural orthopaedic implants, Part I: processing, microstructure, mechanical properties, cytotoxicity, J. Mater. Sci. 19 (2008), 2881-2887.

[10] P. Saravanapavan, J.R. Jones, R. S. Pryce, L.L. Hench, Bioactivity of gel-glass powder in the CaO-SiO$_2$ system: A comparison with ternary (CaO-P$_2$O$_5$-SiO$_2$) and quaternary glasses (SiO$_2$-CaO-P$_2$O$_5$-Na$_2$O), J. Biomed. Mater. Res. Part A 66 (1) (2003) 110-119.

[11] M.N. Rahaman, D.E. Day, B. Sonny Bal, Q. Fu, S.B. Jung, L.F. Bonewald, A.P. Tomsia, Bioaactive glass in tissue engineering, ActaBiomat. 7 (2011) 2355-2373.

[12] L.L. Hench, J. Wilson, Introduction, In. L.L. Hench, J. Wilson (Eds.), Introduction to bioceramics, Singapore: World Scientific, 1993, pp.1-17.

[13] L.L. Hench,J.K. West, Biological applications of bioactive glasses, Life Chem. Rep. 13 (1996) 187-241.

[14] L.L Hench, R.J. Splinter, W.C. Allen, Bonding mechanism at the interface of ceramic prosthetic materials, J. Biomed. Mater. Res. 2 (1971) 117-141.

[15] J.D. Santos, M. Amaral, S.M. Oliveira, M.A. Lopes, R.F. Silva, Silicon Nitride – bioglass[®] 45S5 composite for biomedical applications, Key Eng. Mat. 192-195 (2001) 589-592.

[16] Q.-Z. Chen, Y. Li, L.-Y. Jin, J.M.W. Quinn, P.A. Komesaroff, A new sol-gel process for producing Na$_2$O-containing bioactive glass ceramics, ActaBiomat. 6 (2010) 4143-4153.

[17] O. PeitlFilho, G.P. LaTorre, L.L. Hench, Effect of crystallization on apatite-layer formation of bioactive glass 45S5, J. Biomed. Mater. Res. 30 (1996) 509-514.

[18] O. PeitlFilho, E.D. Zanotto, L.L. Hench, Highly bioactive P$_2$O$_5$ – Na$_2$O – CaO – SiO$_2$ glass ceramics, J. Non.-Cryst. Solid 292 (2001) 115-126.

[19] D.C Clupper, J.J. Mecholsky Jr., G.P. LaTorre, D.C. Greenspan, Sintering temperature effects on the in vivo bioactive response of tape cast and sintered bioactive glass-ceramic in Tris buffer, J. Biomed. Mater. Res. 57 (2001) 532-540.

[20] D.C Clupper, J.J. Mecholsky Jr., G.P. LaTorre, D.C. Greenspan, Bioactivity oftape cast and sintered bioactive glass-ceramic in simulated body fluid, Biomaterials 23(2002) 2599-2606.

[21] T. Kokubo,H. Takadama, How useful is SBF in predicting in vivo bone bioactivity? Biomaterias27 (2006) 2907-2915.

[22] D.C. Clupper, L.L. Hench, Crystallization kinetics of tape cast bioactive glass 45S5, J. Non-Cryst. Solids 318 (2003) 43-48.

[23] S. Hampshire, Silicon nitride ceramics - review of structure, processing and properties, J. Achiev. Mater. Manuf. 24/1 (2007) 43-50.

[24] Y.W. Gu, K.A. Khor, P. Cheang, In vitro studies of plasma-sprayed hydroxyapatite/Ti-6Al-4V composite coatings in simulated body fluid (SBF), Biomaterials 24 (2003) 1603-1611.

[25] L.L Hench, Bioceramics: From concept to clinic, J. Am. Ceram. Soc. 74 (11) (1991) 1487-1510.

[26] P.B. Malafaya, G.A. Silva, R.L. Reis, Natural-origin polymers as carriers and scaffolds for biomolecules and cell delivery in tissue engineering applications, Adv. Drug. Deliver. Rev. 59 (2007) 207-203.

[27] T. Kokubo, H. Kushitani, S. Sakka, T. Kitsugi, T. Yamamuro, Solutions able to reproduce in vivo surface-structure changes in bioactive glass-ceramic A-W, J. Biomed. Mater. Res. 24 (1990) 721-734.

[28] M. Ogino, F. Ohuchi, L.L. Hench, Compositional dependence of the formation of calcium phosphate films on bioglass, J. Biom. Mater. Res. 14 (1980) 55-64.

[29] X. Chatzistavrou, N. Kantiranis, E. Kontonasaki, K. Chrissafis, L. Papadopoulou, P. Koidis, A.R. Boccaccini, K.M. Paraskevopoulos, Thermal analysis and in vivo bioactivity of bioactive glass-alumina composites, Mater. Charact. 62 (2011) 118-129.